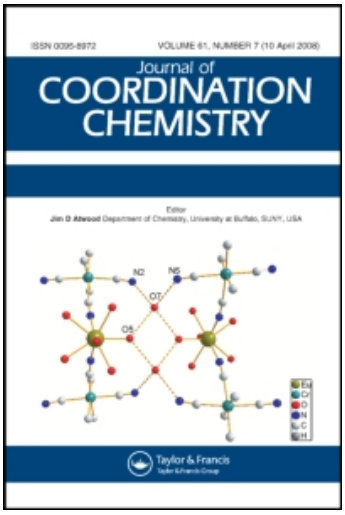

Journal of Coordination Chemistry
Publication details, including instructions for authors and subscription information:
http://www.informaworld.com/smpp/title~content=t713455674

The relationship between ligand structures and their Co^{II} and Ni^{II} complexes: Synthesis and characterization of novel dimeric Co^{II}/Co^{III} complexes of bis(thiosemicarbazone)

H. S. Seleem[a]; A. A. Emara[a]; M. Shebl[a]
[a] Department of Chemistry, Faculty of Education, Ain Shams University, Roxy, Cairo, Egypt

To cite this Article Seleem, H. S. , Emara, A. A. and Shebl, M.(2005) 'The relationship between ligand structures and their Co^{II} and Ni^{II} complexes: Synthesis and characterization of novel dimeric Co^{II}/Co^{III} complexes of bis(thiosemicarbazone)', Journal of Coordination Chemistry, 58: 12, 1003 — 1019
To link to this Article: DOI: 10.1080/00958970500066606
URL: http://dx.doi.org/10.1080/00958970500066606

Journal of Coordination Chemistry
Vol. 58, No. 12, 15 August 2005, 1003–1019

The relationship between ligand structures and their Co^{II} and Ni^{II} complexes: Synthesis and characterization of novel dimeric Co^{II}/Co^{III} complexes of bis(thiosemicarbazone)

H. S. SELEEM*, A. A. EMARA and M. SHEBL

Department of Chemistry, Faculty of Education, Ain Shams University, Roxy, Cairo, Egypt

(*Received 6 July 2004; in final form 26 January 2005*)

4,6-Diacetylresorcinol serves as a starting point for the generation of multidentate S/N/O or O/N/O symmetrical chelating agents by condensation with thiosemicarbazide or semicarbazide to yield the corresponding bis(thiosemicarbazone) H_4L^1 or bis(semicarbazone) H_4L^2, respectively. Reaction of H_4L^1 and H_4L^2 with $M(NO_3)_2 \cdot 6H_2O$ (M = Co or Ni) afforded dimeric complexes for H_4L^1 and binuclear complexes for H_4L^2, revealing the tendency of S to form bridges. The dimeric cobalt complexes of H_4L^1 are very interesting in that they contain Co^{II}/Co^{III}, side/side, low-spin octahedral coordinated Co^{III}-ions and high-spin square-planar coordinated Co^{II}-ions. These complexes have the general formula $[(H_2L^1)_2Co_2(H_2O)(NO_3)] \cdot n$EtOH. Arguments supporting these anomalous Co^{II}/Co^{III} structures are based on a pronounced decrease in their magnetic moments, elemental and thermal analyses, visible and IR spectra, as well as their unreactivity towards organic bases such as 1,10-phenanthroline (phen), 2,2′-bipyridine (Bpy), *N*,*N*,*N*′,*N*′-tetramethylethylenediamine (Tmen) and 8-hydroxyquinoline (oxine, Ox). The dimeric octahedral Ni^{II} complex $[(H_2L^1)_2Ni_2(H_2O)_4] \cdot 3H_2O$ showed higher reactivity towards phen and Bpy and formed adducts; $[(HL^1)Ni_2(B)(H_2O)_5]NO_3$ (B = phen or Bpy). In the presence of oxine, the dimeric brown paramagnetic octahedral complex $[(H_2L^1)_2Ni_2(H_2O)_4] \cdot 3H_2O$ was transformed to the dimeric brick-red diamagnetic square-planar complex $[(H_3L^1)_2Ni_2](NO_3)_2$. The latter showed dramatic behavior in its ^{1}H NMR spectrum in DMSO-d_6, which was explained on the basis of H^+-transfer. By contrast, the binuclear Ni^{II}–H_4L^2 complex (**11**) showed higher reactivity towards phen, Bpy and oxine. These reactions afforded mixed dimeric complexes having the molar ratio 2 : 2 : 1 (Ni^{II} : H_4L^2 : base). The binuclear Co^{II}–H_4L^2 complex afforded an adduct with phen and trinuclear complexes with Bpy and oxine. All complexes were found to be unreactive towards Tmen. Structural characterization was achieved by elemental and thermal analyses, spectral data (electronic, IR, mass and ^{1}H NMR spectra) and conductivity and magnetic susceptibility measurements.

Keywords: Binuclear; Trinuclear; Adducts; Dimeric and mixed dimeric Co^{II}/Co^{III} and Ni^{II} complexes; Bis(thiosemicarbazone); Bis(semicarbazone)

*Corresponding author. Email: hsseleem@yahoo.com

Journal of Coordination Chemistry
ISSN 0095-8972 print: ISSN 1029-0389 online © 2005 Taylor & Francis Group Ltd
DOI: 10.1080/00958970500066606

1. Introduction

Thiosemicarbazone and semicarbazone derivatives comprise an intriguing class of chelating molecules. Their complexes possess a wide range of beneficial medicinal and pharmaceutical activities [1–6]. We report here the syntheses, structures and properties of a novel series of Ni^{II}, Co^{II} and Co^{II}/Co^{III} complexes of bis(thiosemicarbazones) and bis(semicarbazones) derived from 4,6-diacetylresorcinol. This study is a continuation of our work on hydrazones [4–9] and thiosemicarbazones [10].

2. Experimental

All chemicals, metal nitrates and solvents were either Aldrich, BDH or Merck products. FTIR spectra were recorded on a Perkin Elmer FTIR 1650 spectrometer (4000–200 cm^{-1}) using KBr pellets. Electronic spectra were recorded at room temperature on a Jasco model V-550 UV/vis spectrophotometer as Nujol mulls and/or solutions in DMF. ^1H NMR spectra of the ligands and some complexes, as solutions in DMSO-d_6, were recorded on a Bruker WP 200 SY spectrometer at room temperature using TMS as internal standard. Mass spectra were recorded at 290°C and 70 eV on a Hewlett-Packard MS-5988 mass spectrometer. Molar conductivities of 10^{-3} M solutions of the solid complexes in DMF were measured on a Corning conductivity meter NY 14831 model 441. Magnetic susceptibilities of the complexes were measured by the Gouy method at room temperature using a Johnson Matthey, Alfa Products, model MKI magnetic susceptibility balance. The effective magnetic moments were calculated from the expression $\mu_{eff} = 2.828(\chi_M T)^{1/2}$ BM, where χ_M is the molar susceptibility corrected using Pascal's constants for the diamagnetism of all atoms in the compounds. Carbon, hydrogen, nitrogen and sulfur microanalyses were carried out at the Microanalysis Center, Cairo University, Giza, Cairo, Egypt. TG-DSC analysis was carried out on a Shimadzu-50 thermal analyzer at a heating rate of 10°C/min in a nitrogen atmosphere (30 mL/min) over the temperature range 20–800°C. The melting points of the complexes were determined using a RUMO melting point apparatus, model 3600.

2.1. *Preparation of H_4L^1 and H_4L^2 ligands*

A mixture of 4,6-diacetylresorcinol (0.01 mol) and thiosemicarbazide or semicarbazide hydrochloride (0.02 mol) dissolved in a minimum amount of water was refluxed for 4 h to yield H_4L^1 and H_4L^2 ligands, respectively. The reaction mixture was cooled and the solid formed was filtered off, washed with water, ethanol and finally ether and crystallized from DMF–water. Analytical and physical data for the ligands are shown in table 1.

2.2. *Preparation of the metal complexes*

The following detailed preparations are given as examples and the other complexes were obtained similarly.

Table 1. Analytical and physical data for the ligands and their metal complexes.

No.	Reaction	Complex MF [FW]	Color	Yield (%)	Elemental analysis % Found/(Calc.) C	H	N	S	M
	H_4L^1	$C_{12}H_{16}N_6O_2S_2$ [340.43]	Pale yellow	77	42.40 (42.34)	4.80 (4.74)	24.35 (24.69)	18.68 (18.84)	–
1	$H_4L^1 + Ni(NO_3)_2 \cdot 6H_2O$	$[(H_2L^1)_2Ni_2(H_2O)_4] \cdot 3H_2O$ ($C_{24}H_{42}N_{12}O_{11}S_4Ni_2$) [920.35]	Brown	39	31.10 (31.32)	4.40 (4.60)	18.50 (18.26)	14.10 (13.94)	12.60 (12.76)
2	$H_4L^1 + Ni(NO_3)_2 \cdot 6H_2O + Ox$	$[(H_3L^1)_2Ni_2](NO_3)_2$ ($C_{24}H_{30}N_{14}O_{10}S_4Ni_2$) [920.27]	Brick red	36	31.70 (31.32)	3.30 (3.29)	20.97 (21.31)	14.08 (13.94)	12.60 (12.76)
3	$H_4L^1 + Ni(NO_3)_2 \cdot 6H_2O + phen$	$[(HL^1)Ni_2(phen)(H_2O)_5]NO_3$ ($C_{24}H_{31}N_9O_{10}S_2Ni_2$) [787.12]	Brown	60	36.50 (36.62)	4.00 (3.97)	16.18 (16.02)	7.86 (8.15)	14.70 (14.92)
4	$H_4L^1 + Ni(NO_3)_2 \cdot 6H_2O + Bpy$	$[(HL^1)Ni_2(Bpy)(H_2O)_5]NO_3 \cdot 1\frac{1}{2}EtOH$ ($C_{25}H_{40}N_9O_{11.5}S_2Ni_2$) [832.20]	Brown	54	36.00 (36.08)	4.60 (4.84)	15.43 (15.15)	7.42 (7.71)	13.90 (14.11)
5	$H_4L^1 + Ni(NO_3)_2 \cdot 6H_2O + Tmen$	$[(H_2L^1)_2Ni_2(H_2O)_4] \cdot 2\frac{1}{2}EtOH$ ($C_{29}H_{51}N_{12}O_{10.5}S_4Ni_2$) [981.48]	Brownish-yellow	39	35.55 (35.49)	5.24 (5.24)	16.87 (17.13)	13.32 (13.07)	11.80 (11.96)
6	$H_4L^1 + Co(NO_3)_2 \cdot 6H_2O$	$[(H_2L^1)_2Co_2(H_2O)_2]NO_3 \cdot 5H_2O$ ($C_{24}H_{42}N_{13}O_{14}S_4Co_2$) [964.79]	Brown	41	29.10 (29.30)	4.50 (4.27)	18.78 (18.52)	12.85 (13.02)	11.90 (11.99)
7	$H_4L^1 + Co(NO_3)_2 \cdot 6H_2O + Ox$	$[(H_2L^1)_2Co_2(H_2O)(NO_3)]EtOH$ ($C_{26}H_{36}N_{13}O_9S_4Co_2$) [920.78]	Brown	38	33.72 (33.92)	3.88 (3.94)	19.54 (19.78)	14.23 (13.93)	12.60 (12.80)
8	$H_4L^1 + Co(NO_3)_2 \cdot 6H_2O + phen$	$[(H_2L^1)_2Co_2(H_2O)(NO_3)]1\frac{1}{2}EtOH$ ($C_{27}H_{39}N_{13}O_{9.5}S_4Co_2$) [943.82]	Brown	36	34.39 (34.36)	4.11 (4.17)	19.65 (19.29)	13.30 (13.59)	12.30 (12.49)
9	$H_4L^1 + Co(NO_3)_2 \cdot 6H_2O + Bpy$	$[(H_2L^1)_2Co_2(H_2O)(NO_3)]1\frac{1}{4}EtOH$ ($C_{26.5}H_{37.5}N_{13}O_{9.25}S_4Co_2$) [932.30]	Brown	35	34.10 (34.14)	4.53 (4.05)	19.21 (19.53)	13.41 (13.76)	12.50 (12.64)
10	$H_4L^1 + Co(NO_3)_2 \cdot 6H_2O + Tmen$	$[(H_2L^1)_2Co_2(H_2O)(NO_3)]2EtOH$ ($C_{28}H_{42}N_{13}O_{10}S_4Co_2$) [966.85]	Brown	44	35.00 (34.78)	4.23 (4.38)	18.40 (18.83)	12.90 (13.27)	12.00 (12.19)
	H_4L^2	$C_{12}H_{16}N_6O_4$ [308.30]	Yellowish-orange	75	46.50 (46.75)	5.00 (5.23)	27.01 (27.26)		–
11	$H_4L^2 + Ni(NO_3)_2 \cdot 6H_2O$	$[(H_2L^2)Ni_2(H_2O)_5(NO_3)_2]\frac{1}{4}EtOH$ ($C_{12.5}H_{25.5}N_8O_{15.25}Ni_2$) [649.31]	Pale brown	95	23.04 (23.12)	4.44 (3.96)	16.90 (17.26)		18.10 (18.08)
12	$H_4L^2 + Ni(NO_3)_2 \cdot 6H_2O + Ox$	$[(H_2L^2)(H_3L^2)Ni_2(Ox)(H_2O)_3] \cdot 2\frac{1}{2}H_2O$ ($C_{33}H_{46}N_{13}O_{14.5}Ni_2$) [974.23]	Pale brown	79	40.47 (40.69)	4.96 (4.76)	18.24 (18.69)		11.90 (12.05)
13	$H_4L^2 + Ni(NO_3)_2 \cdot 6H_2O + phen$	$[(H_2L^2)(H_3L^2)Ni_2(phen)(NO_3)(EtOH)(H_2O)]$ $EtOH(C_{40}H_{51}N_{15}O_{14}Ni_2)$ [1083.36]	Pale brown	69	44.51 (44.35)	4.82 (4.75)	18.94 (19.39)		10.70 (10.84)

(*continued*)

Table 1. Continued.

No.	Reaction	Complex MF [FW]	Color	Yield (%)	Elemental analysis % Found/(Calc.) C	H	N	S	M
14	$H_4L^2 + Ni(NO_3)_2 \cdot 6H_2O + Bpy$	$[(H_2L^2)(H_3L^2)Ni_2(Bpy)(NO_3)(H_2O)_2] \cdot 2\frac{1}{2}H_2O$ ($C_{34}H_{46}N_{15}O_{15.5}Ni_2$) [1030.26]	Pale brown	65	39.61 (39.64)	4.82 (4.50)	19.97 (20.39)		11.30 (11.40)
15	$H_4L^2 + Ni(NO_3)_2 \cdot 6H_2O + Tmen$	$[(H_2L^2)Ni_2(H_2O)_5(NO_3)_2]EtOH$ ($C_{14}H_{30}N_8O_{16}Ni_2$) [683.86]	Pale brown	80	24.60 (24.59)	4.43 (4.42)	16.00 (16.39)		17.00 (17.17)
16	$H_4L^2 + Co(NO_3)_2 \cdot 6H_2O + LiOH$	$[(H_2L^2)Co_2(H_2O)_5(NO_3)_2]\frac{1}{2}EtOH$ ($C_{13}H_{27}N_8O_{15.5}Co_2$) [661.27]	Deep brown	89	23.51 (23.61)	4.25 (4.12)	16.71 (16.95)		17.60 (17.82)
17	$H_4L^2 + Co(NO_3)_2 \cdot 6H_2O +$ $Ox + LiOH$	$[(H_2L^2)_2Co_3(OH)_2]EtOH$ ($C_{26}H_{36}N_{12}O_{11}Co_3$) [869.45]	Deep olive-green	56	35.80 (35.92)	4.50 (4.17)	18.92 (19.33)		20.10 (20.33)
18	$H_4L^2 + Co(NO_3)_2 \cdot 6H_2O +$ $phen + LiOH$	$[(HL^2)Co_2(phen)NO_3(H_2O)_4] \cdot 2H_2O \cdot EtOH$ ($C_{26}H_{39}N_9O_{14}Co_2$) [819.52]	Deep brown	88	38.00 (38.11)	4.80 (4.80)	15.71 (15.38)		14.00 (14.38)
19	$H_4L^2 + Co(NO_3)_2 \cdot 2.5H_2O +$ $Bpy + LiOH$	$[(H_2L^2)_2Co_3(H_2O)_4(OH)_2]1\frac{1}{2}EtOH$ ($C_{27}H_{47}N_{12}O_{15.5}Co_3$) [964.55]	Brown	56	33.69 (33.62)	4.81 (4.91)	17.20 (17.43)		18.10 (18.33)
20	$H_4L^2 + Co(NO_3)_2 \cdot 6H_2O +$ $Tmen + LiOH$	$[(H_2L^2)Co_2(H_2O)_5(NO_3)_2]H_2O$ ($C_{12}H_{26}N_8O_{16}Co_2$) [656.25]	Brown		21.90 (21.96)	4.40 (3.99)	17.30 (17.07)		17.70 (17.96)

2.2.1. Preparation of the $[(H_3L^1)_2Ni_2(H_2O)_4]\cdot 3H_2O$ complex. An ethanolic solution (40 mL) of $Ni(NO_3)_2\cdot 6H_2O$ (1.37 g, 4.7 mmol) was added gradually to a suspension of the ligand (H_4L^1) in ethanol (40 mL) (0.8 g, 2.35 mmol). The mixture was refluxed for 5 h and a brown precipitate was formed. The precipitate was filtered, washed with ethanol, then diethylether and finally air-dried. Yield 0.34 g (39%).

2.2.2. Preparation of mixed-ligand complexes (adducts). An ethanolic solution (40 mL) of $Ni(NO_3)_2\cdot 6H_2O$ or $Co(NO_3)_2\cdot 6H_2O$ was added gradually to a suspension of the ligands (H_4L^1 and H_4L^2) in ethanol (40 mL) in the molar ratio 2 : 1 (M : L). The mixture was refluxed for 30 min and then an ethanolic solution of 8-hydroxyquinoline (oxine, Ox), 1,10-phenanthroline (phen), 2,2′-bipyridyl (Bpy) or *N*,*N*,*N*′,*N*′-tetramethylethylenediamine (Tmen) was added to give a metal ion : ligand : base molar ratio of 2 : 1 : 2. The solution was refluxed for 5 h, during which time the solid complexes precipitated out. These precipitates were filtered, washed with ethanol and then diethylether and finally air-dried.

3. Results and discussion

3.1. *The ligands*

The structures of the ligands were elucidated by elemental analysis, electronic, IR and ^{1}H NMR spectroscopy. The results of the elemental analyses (table 1) are in good agreement with the proposed formulae. The thiosemicarbazone (H_4L^1) and the semicarbazone (H_4L^2) ligands exist in tautomeric thione/keto and thiol/enol forms.

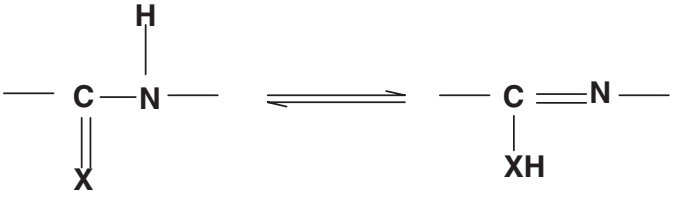

(X = S; H_4L^1 or O; H_4L^2)

IR spectra of the ligands (table 2) showed broad bands at 2922 and 2885 cm^{-1} assigned to ν(OH···N) (phenolic group), strong bands at 1618 and 1623 cm^{-1} attributed to ν(C=N), and very strong bands at 3188 and 3206 cm^{-1} assigned to ν(NH) of both H_4L^1 and H_4L^2, respectively. Two strong bands at 3405 and 3450 and at 3300 and 3350 cm^{-1} are assigned to ν_{as} and ν_s of the –NH_2 group of H_4L^1 and H_4L^2, respectively. As both ligands contain the –NHC=X grouping [X = S(H_4L^1) and O(H_4L^2)], they showed amide group vibrations [11], respectively, at around (i) 1551 and 1671 cm^{-1} [amide I; ν(C=S) and ν(C=O)], (ii) 1270 and 1274 cm^{-1} [amide II; ν(C–N) + δ(N–H)], (iii) 1044 and 1067 cm^{-1} [amide III; δ(N–H)], and (iv) 778 and 815 cm^{-1} [amide IV; ϕ(C=S) and ϕ(C=O)].

Table 2. IR spectral data of the ligand H_4L^1 and its metal complexes.

No.	Complex	IR spectral bands (cm^{-1}) νOH H_2O/EtOH/phenolic	νC=N free	νC=N coord	νC=S Amide	νC–S	Other bands
	H_4L^1	2922	1618	–	1551	–	3405 ν_{as}, 3300 $\nu_s(NH_2)$ −3188; ν(NH) −1270, 1044, 778; ν(amide II, III, IV, resp.)
1	$[(H_2L^1)_2Ni_2(H_2O)_4]\cdot 3H_2O$	3369	1622	1600	1534	790	
2	$[(H_3L^1)_2Ni_2](NO_3)_2$	3327	1622	1602	1525	792	1374; $\nu(NO_3^-)$
3	$[(HL^1)Ni_2(phen)(H_2O)_5]NO_3$	3360	1618	1599	–	776	1374; $\nu(NO_3^-)$ 1490; νC=N(phen)
4	$[(HL^1)Ni_2(Bpy)(H_2O)_5]NO_3\cdot 1\frac{1}{2}EtOH$	3363	1617	1600	–	780	1372; $\nu(NO_3^-)$ 1493; νC=N(Bpy)
5	$[(H_2L^1)_2Ni_2(H_2O)_4]\cdot 2\frac{1}{2}EtOH$	3370	1621	1597	1536	793	
6	$[(H_2L^1)_2Co_2(H_2O)_2]\ NO_3\cdot 5H_2O$	3381	1620	1590	1540	789	1373; $\nu(NO_3^-)$
7	$[(H_2L^1)_2Co_2(H_2O)(NO_3)]\cdot EtOH$	3400	1619	1589	1538	790	1424 (ν_5); $\nu_{as}(NO_2)$ 1377 (ν_1); $\nu_s(NO_2)$
8	$[(H_2L^1)_2Co_2(H_2O)(NO_3)]\cdot 1\frac{1}{2}$ EtOH	3407	1622	1588	1536	778	1422 (ν_5); $\nu_{as}(NO_2)$ 1376 (ν_1); $\nu_s(NO_2)$
9	$[(H_2L^1)_2Co_2(H_2O)(NO_3)]\cdot 1\frac{1}{4}$ EtOH	3400	1621	1589	1540	788	1420 (ν_5); 1377 (ν_1) of the NO_3^- (C_{2v} group)
10	$[(H_2L^1)_2Co_2(H_2O)(NO_3)]\cdot 2EtOH$	3369	1618	1598	1534	796	1423 (ν_5); $\nu_{as}(NO_2)$ 1376 (ν_1); $\nu_s(NO_2)$
		νOH H_2O/EtOH/phenolic	νC=O Amide I	νC=N free	νC=N coord.		
	H_4L^2	2885	1671	1623	–		3450 ν_{as}, 3350 $\nu_s(NH_2)$ –3206; ν(NH) −1274, 1067, 815; ν(amide II, III, IV, resp.)
11	$[(H_2L^2)Ni_2(H_2O)_5(NO_3)_2]\cdot\frac{1}{4}$ EtOH	3381	1651	1625	1590		1419 (ν_5); $\nu_{as}(NO_2)$ 1383 (ν_1); $\nu_s(NO_2)$
12	$[(H_2L^2)(H_3L^2)Ni_2(Ox)(H_2O)_3]\cdot 2\frac{1}{2}H_2O$	3395	1663	1627	1589		1500; νC=N(oxine)
13	$[(H_2L^2)(H_3L^2)Ni_2(phen)(NO_3)(EtOH)(H_2O)]\cdot EtOH$	3351	1663	1627	1589		1420 (ν_5); 1380 (ν_1) M–NO_3 1528; νC=N(phen)
14	$[(H_2L^2)(H_3L^2)Ni_2(Bpy)(NO_3)(H_2O)_2]\cdot 2\frac{1}{2}H_2O$	3361	1675	1625	1598		1440 (ν_5); 1370 (ν_1) M–NO_3 1537; νC=N(Bpy)
15	$[(H_2L^2)Ni_2(H_2O)_5(NO_3)_2]\cdot EtOH$	3400	1655	1627	1597		1421 (ν_5); ν_{as} (NO_2) M–NO_3 1379 (ν_1); (ν_5) (NO_2)
16	$[(H_2L^2)Co_2(H_2O)_5(NO_3)_2]\cdot\frac{1}{2}EtOH$	3396	1653	1627	1588		1432 (ν_5); $\nu_{as}(NO_2)$ M–NO_3 1373 (ν_1); (ν_5) (NO_2)
17	$[(H_2L^2)_2Co_3(OH)_2]\cdot EtOH$	3388	–	1625	1587		
18	$[(HL^2)Co_2(phen)NO_3(H_2O)_4]2H_2O\cdot EtOH$	3334	–	1625	1587		1427; (ν_5); 1384(ν_1) 1514; νC=N(phen)
19	$[(H_2L^2)_2Co_3(H_2O)_4(OH)_2]\cdot 1\frac{1}{2}EtOH$	3347	–	1626	1589		
20	$[(H_2L^2)Co_2(H_2O)_5(NO_3)_2]\cdot H_2O$	3360	1655	1624	1599		1440 (ν_5); $\nu_{as}(NO_2)$ 1379 (ν_1); $\nu_s(NO_2)$

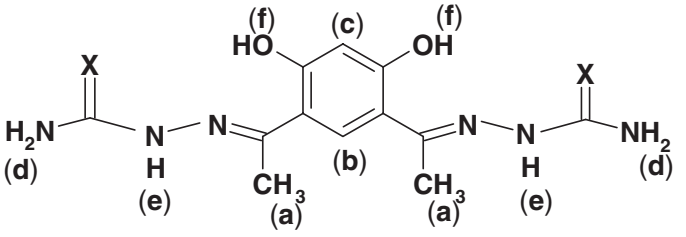

	δ (ppm)					
	H^a	H^b	H^c	H^d	H^e	H^f
H_4L^1 (X = S)	2.35 (6H)	6.35 (1H)	7.64 (1H)	7.98 (4H)	10.25 (2H)	12.62 (2H)
H_4L^2 (X = O)	2.27 (6H)	6.27 (1H)	7.53 (1H)	7.99 (4H)	9.57 (2H)	11.65 (2H)

Scheme 1. ^{1}H NMR spectra of the ligands in DMSO-d_6.

These bands support the ketonic nature (thione/keto form) of the ligands in the solid state. The absence of an IR band around 2600 cm^{-1} due to ν(SH) supports the thione nature of the H_4L^1 ligand in the solid state [12]. In addition, the absence of a signal at *ca.* 4.0 ppm in the ^{1}H NMR spectra attributable to the SH proton provides strong evidence of the thione form of H_4L^1 even in the solution state [12].

Electronic spectra of the ligands in DMF showed bands in the ranges 225–273, 297–300 and 333–345 nm. The higher energy bands in the region 225–273 nm are assigned to π–π* transitions of the azomethine linkage and the aromatic benzene ring. The medium energy bands in the region 297–300 nm are assigned to n–π* transitions of the C=O, C=N and C=S groups. Finally, the lower energy bands in the region 333–345 nm are attributed to charge transfer (CT) transitions within the molecules.

^{1}H NMR spectral data (δ ppm) of the ligands relative to TMS (0 ppm) in DMSO-d_6 lend further support to the suggested structures of the ligands (scheme 1). All peaks were recorded as singlets and are exchangeable with D_2O except the methyl and aromatic protons. These data, together with the data derived from the elemental analysis, IR and electronic spectra, confirmed the structures given for these ligands.

3.2. *The metal complexes*

All of the complexes are stable at room temperature, nonhygroscopic and insoluble in water and alcohols with colors ranging from olive green to dark brown. The melting points of both ligands and their complexes are above 300°C. Characterization and structure elucidation of the solid metal complexes were carried out by elemental and thermal (TG-DSC) analyses, spectral data (UV–Vis, IR, ^{1}H NMR and mass spectra) as well as conductivity and magnetic susceptibility measurements.

Reaction of the bis(carbazone) ligands with transition metal ions can proceed via the phenolic oxygen and azomethine nitrogen, in addition to one of the following: (i) thione sulfur (C=S) or carbonyl oxygen (C=O), (ii) thiol sulfur or enolic oxygen, (iii) both i and ii, that is thione–thiol sulfurs or keto–enol oxygens in the same complex, and (iv) the terminal amino (–NH_2) group. The latter pathway was excluded on the basis of IR and ^{1}H NMR spectral data. The ligands H_4L^1 and H_4L^2 are tetrabasic and

have two sets of SNO and ONO donor sites; therefore, they were allowed to react with all metal ions in the molar ratio 2 : 1 (metal : ligand). The elemental analyses (table 1) agreed with the proposed formulas.

The bis(carbazone) ligands H_4L^1 and H_4L^2 were allowed to react with Co^{II} and Ni^{II} nitrates in the absence and presence of phen, Bpy, Tmen and oxine. These reactions afforded dimeric complexes (scheme 4; complexes **1**, **2**, **5**–**10**) for H_4L^1. By contrast, binuclear complexes (scheme 6; complexes **11**, **15**, **16**, **20**) and trinuclear Co^{II} complexes (scheme 7; complexes **17**, **19**) as well as mixed dimeric Ni^{II} complexes (scheme 4; complexes **12**–**14**) were obtained for H_4L^2. These reactions afforded adducts for both ligands having the molar ratio 2 : 1 : 1 (Co^{II}/Ni^{II} : ligand : phen/Bpy) (scheme 5; complexes **3**, **4**, **18**). The stereochemical diversity and the various structural possibilities in addition to the variety of modes of bonding are attributed to the different tautomeric structures of the ligands H_4L^1 and H_4L^2 and the greater tendency of both S and O donors to form bridges. All attempts to isolate adducts with OO donors, such as benzil or 2-hydroxyacetophenone, were unsuccessful, as were attempts to isolate mononuclear complexes.

3.3. *Conductivity measurements*

The molar conductance of 1×10^{-3} mol dm^{-3} solutions of the metal complexes in DMF were measured at room temperature and the results are listed in table 3. The molar conductance values reveal that (i) all the semicarbazone H_4L^2 complexes are nonelectrolytes and (ii) the thiosemicarbazone H_4L^1 complexes can be classified into three categories: 1 : 1 electrolytes (complexes **3**, **4**, **6**), 2 : 1 electrolytes (complex **2**) and nonelectrolytes (the others). For the 1 : 1 and 2 : 1 electrolytes, the NO_3^- anions are outside the metal coordination sphere (complexes **2**–**4**, **6**).

3.4. *IR spectra of the metal complexes*

The IR spectra of the ligands and their metal complexes (table 2) are mainly characterized by NH_2, OH···N, C=O, C=N and C=S vibrational modes. Comparison of the IR spectra of the metal complexes with those of the free ligands revealed that all complexes showed a broad band around 3407–3327 cm^{-1} assignable to νOH of the coordinated water molecules. The broad band around 2900 cm^{-1} attributable to ν(OH···N) intramolecular H-bonding of the phenolic group in the free ligands disappeared on complexation, indicating the replacement of the phenolic proton by the metal ions and/or overlapped with ν(OH) of the coordinated water molecules. In addition, the two strong bands around 3400 and 3300 cm^{-1} assigned to ν_{as} and ν_s of the $-NH_2$ group, respectively, in the free ligands remained intact in all complexes, indicating nonparticipation of the $-NH_2$ group in chelation. The two strong bands at 1618 and 1623 cm^{-1} assigned to ν(C=N) for $H_4L^1$and H_4L^2, respectively, were shifted to lower wave numbers in all complexes indicating participation of the azomethine nitrogen in chelation. The disappearance of the amide band I and the splitting of ν(C=N) band into two bands at 1627–1617 and 1602–1587 cm^{-1} due to free and coordinated C=N groups, respectively, provides strong evidence that the enolic S/O participates in chelation after deprotonation leading to a covalent linkage. On the other hand, the appearance of two new bands around 1440–1419 (ν_5) and 1384–1373 cm^{-1} (ν_1) in complexes **7**–**11**, **13**–**16**, **18** and **20** confirmed monodentate

Table 3. Electronic spectra, magnetic moments and molar conductivity data of H_4L^1 and its metal complexes.

No.	Complex	Electronic spectral bands (nm)	μ_{eff}[a] (BM)	μ_{compl}[b] (BM)	Conductance[c] ($ohm^{-1}\ cm^2\ mol^{-1}$)
	H_4L^1	227, 249, 273, 297, 345	–	–	–
1	$[(H_2L^1)_2Ni_2(H_2O)_4]\cdot 3H_2O$	355, 384, 425, 454, 482	2.0	2.73	43
2	$[(H_3L^1)_2Ni_2](NO_3)_2$	395, 415, 485	Diam.	Diam.	170
3	$[(HL^1)Ni_2(phen)(H_2O)_5]NO_3$	355, 385, 425, 454, 482, 494	2.15	2.85	100
4	$[(HL^1)Ni_2(Bpy)(H_2O)_5]NO_3\cdot 1\frac{1}{2}$ EtOH	354, 373, 392, 425, 453, 473	2.20	2.99	70
5	$[(H_2L^1)_2Ni_2(H_2O)_4]\cdot 2\frac{1}{2}$ EtOH	390, 424, 450, 487	2.0	2.70	41
6	$[(H_2L^1)_2Co_2(H_2O)_2]NO_3\cdot 5H_2O$	426	2.0	2.0	84
7	$[(H_2L^1)_2Co_2(H_2O)(NO_3)]\cdot$ EtOH	426	2.40	2.40	41
8	$[(H_2L^1)_2Co_2(H_2O)(NO_3)]\cdot 1\frac{1}{2}$ EtOH	426	2.30	2.30	33
9	$[(H_2L^1)_2Co_2(H_2O)(NO_3)]\cdot 1\frac{1}{4}$ EtOH	426	2.33	2.33	27
10	$[(H_2L^1)_2Co_2(H_2O)(NO_3)]\cdot 2$ EtOH	356, 376, 424	2.40	2.40	21
	H_4L^2	225, 249, 273, 300, 333	–	–	–
11	$[(H_2L^2)Ni_2(H_2O)_5(NO_3)_2]\cdot\frac{1}{4}$ EtOH	(390, 480, 547)[d]	3.31	4.69	insol.
12	$[(H_2L^2)(H_3L^2)Ni_2(Ox)(H_2O)_3]\cdot 2\frac{1}{2}H_2O$	390, 421 and (366, 455, 520)[d]	3.03	4.19	10
13	$[(H_2L^2)(H_3L^2)Ni_2(phen)(NO_3)(EtOH)(H_2O)]\cdot$ EtOH	380 and (361, 402)[d]	2.83	3.88	7.0
14	$[(H_2L^2)(H_3L^2)Ni_2(Bpy)(NO_3)(H_2O)_2]\cdot 2\frac{1}{2}H_2O$	394 and (420, 530)[d]	3.0	4.15	5.0
15	$[(H_2L^2)Ni_2(H_2O)_5(NO_3)_2]\cdot$ EtOH	378 and (398, 500, 600)[d]	3.32	4.64	4.0
16	$[(H_2L^2)Co_2(H_2O)_5(NO_3)_2]\cdot\frac{1}{2}$ EtOH	(363, 500)[d]	3.80	5.30	insol.
17	$[(H_2L^2)_2Co_3(OH)_2]\cdot$ EtOH	421 and (392, 490, 600)[d]	2.38	3.98	3.0
18	$[(HL^2)Co_2(phen)NO_3(H_2O)_4]2H_2O\cdot$ EtOH	380 and (600)[d]	3.42	4.69	10
19	$[(H_2L^2)_2Co_3(H_2O)_4(OH)_2]\cdot 1\frac{1}{2}$ EtOH	392 and (500)[d]	2.84	4.75	7.0
20	$[(H_2L^2)Co_2(H_2O)_5(NO_3)_2]\cdot H_2O$	374 and (600)[d]	3.92	5.48	4.0

[a]μ_{eff} is the magnetic moment of one cationic species in the complex.
[b]μ_{compl} is the total magnetic moment of all cations in the complex.
[c]Solutions in DMF (10^{-3} M).
[d]Nujol mull.

NO_3^- (C_{2v} symmetry) [13]. As expected for C_{2v} symmetry, these two NO stretching bands are assigned to $\nu_{as}(NO_2)$ and $\nu_s(NO_2)$, respectively. In electrolytic complexes **2**–**4** and **6**, the NO_3^- anion showed a new band around 1374–1372 cm^{-1} confirming its ionic nature [13]. The mixed-ligand adducts **3**, **4**, **12**–**14** and **18** had new bands around 1537–1490 cm^{-1}, attributed to coordinated C=N of the heterocyclic aromatic base (phen, Bpy or oxine), indicating N-coordination of the base [13,14]. Support for the above interpretation is found in the appearance of non-ligand bands; of the several bands observed in the far-IR spectra, non-ligand bands were observed at 560–400 [ν(M–O)], 400–320 [ν(M–N)] and 320–260 cm^{-1} [ν(M–S)].

3.5. *^{1}H NMR spectra*

^{1}H NMR spectra of the ligands and the diamagnetic, square-planar Ni^{II} complex $[(H_3L^1)_2Ni_2](NO_3)_2$ (**2**) were recorded in DMSO-d_6. The data and their assignments are listed in schemes 1 and 2. The ^{1}H NMR spectrum of the diamagnetic Ni^{II} complex **2** showed unexpected behavior, which could be explained on the basis of proton transfer from the chelated OH to the free NH_2 group in the same molecule. This proton transfer changes the chemical environment, as can be represented by the equilibria shown in scheme 2. This is not surprising given that (i) H^+-transfer can

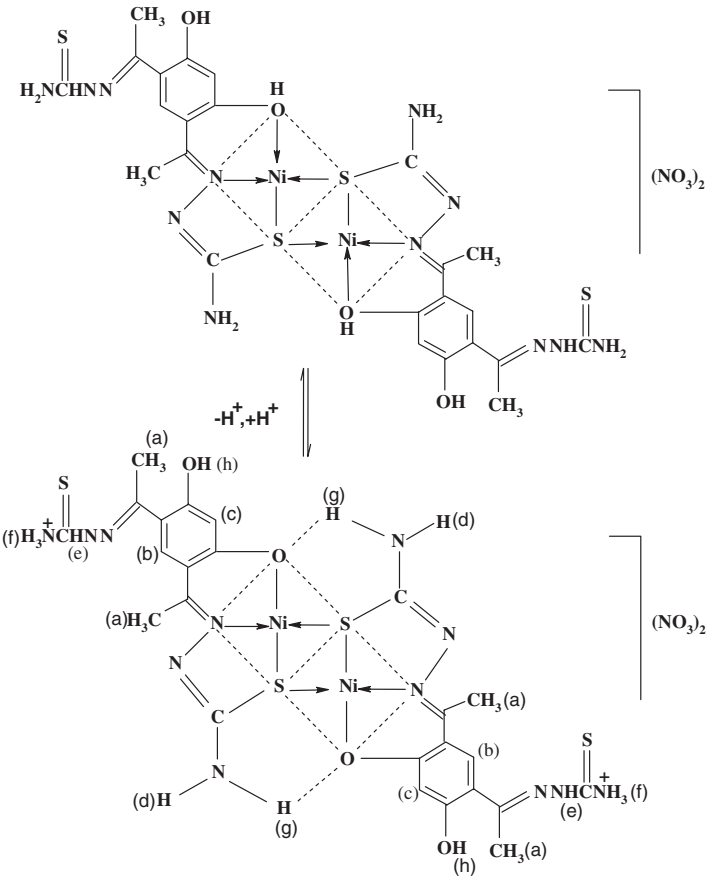

δ (ppm)							
H^a	H^b	H^c	H^d	H^e	H^f	H^g	H^h
2.23 (12H)	5.6 (2H)	7.66 (2H)	8.16 (2H)	8.84 (2H)	9.78 (6H)	10.60 (2H)	11.86 (2H)

Scheme 2. ^{1}H NMR spectrum of square planar $[(H_3L^1)_2Ni_2](NO_3)_2$ (**2**) in DMSO-d_6.

easily occur in polar solvents such as DMSO-d_6 or DMF. The latter accounts for the high value of the molar conductance of the Ni^{II} complex **2** ($170\,\Omega^{-1}\,cm^2\,mol^{-1}$; see table 3). (ii) H^+-transfer can also occur readily because of the presence of both a chelated phenolic (OH) group, which can lose a proton, and an $-NH_2$ group (sp^3-hybridization), which can accept the lost proton. (iii) This H^+-transfer leads to the formation of two six-membered rings by H-bonding (scheme 2), providing more structural stabilization. (iv) Such proton transfer has been observed by other authors [15–18] on studies on the complexation of Schiff bases derived from 2,6-diformyl-4-X-phenol (X = Me, *t*Bu, OMe). On examining the ^{1}H NMR spectrum of the diamagnetic square-planar Ni^{II} complex **2** in comparison to that of the free H_4L^1 ligand, we can conclude that: (i) the aromatic protons in position 5 and the phenolic protons underwent upfield shifts (shifts to lower δ values) on complexation, whereas

(ii) the NH_2 and NH protons underwent downfield shifts (shifts to higher δ values). (iii) In addition, new signals appeared as a result of complexation and their assignments are presented in scheme 2. (iv) Finally, the methyl protons are almost unaffected. All signals were recorded as singlets and are exchangeable with D_2O except those assigned to methyl and aromatic protons.

3.6. *Visible spectra and magnetochemistry*

Visible spectra of the metal complexes (table 3) were measured as DMF solutions and/or Nujol mulls, as some of the metal complexes were sparingly soluble in most common solvents. Comparison of the spectra of the free ligands and their complexes showed the persistence of the ligand bands in all complexes. The bands of the free ligands were slightly shifted to blue or red regions of the spectrum in all complexes, and new bands were observed in the visible region due to d–d transitions (table 3). CT transitions are of higher energy than d–d transitions and usually lie at the extreme blue end of the visible spectrum or in the ultraviolet region.

3.7. *Cobalt complexes*

Magnetic properties can distinguish the stereochemistry of Co^{II} complexes, as T_d complexes have three unpaired electrons and square planar complexes only one. The magnetic moments, μ_{eff}, of Co^{II}–H_4L^2 complexes (**16**–**20**) lie in the range 2.38–3.92 BM, which is higher than for square planar geometry and lower than either T_d or O_h geometries, especially for trinuclear complexes **17** and **19** (table 3). These low values indicate strong antiferromagnetic exchange between adjacent Co^{II}-ions. However, this range is generally found for high-spin O_h cobaltous complexes. This observation is compatible with their electronic spectra; a shoulder at 500 or 600 nm (table 3) would be due to $^4T_{1g}(F) \rightarrow {}^4A_{2g}(F)$ ν_2 transition in O_h-geometry. The $^4T_{1g}(F) \rightarrow {}^4T_{1g}(P)$ ν_3 transition is not observed as it is overlapped by CT and intraligand transitions. Also, the $^4T_{1g}(F) \rightarrow {}^4T_{2g}(F)$ ν_1 transition is not observed in the near-IR region.

The dimeric cobalt–H_4L^1 complexes (**6**–**10**) showed anomalous behavior with magnetic moments in the range 2.0–2.4 BM, indicative of one unpaired electron and square planar geometry around Co^{II}. Their visible spectra showed one band at 23,474 cm^{-1}, which is consistent with ν_2 transition; $^1A_{1g} \rightarrow {}^1T_{2g}$ assigned for Co^{III}(d^6-system) in low-spin O_h-geometry [19]. These dimeric complexes can be represented by the following general skeleton, containing side-by-side, low-spin O_h coordinated Co^{III}-ions and high-spin square-planar coordinated Co^{II}-ions.

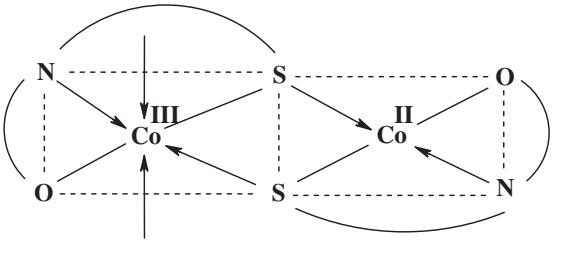

The unpaired electron occupies the d_z^2 orbital as expected. Arguments supporting these Co^{II}/Co^{III} structures begin with the observation that a pronounced decrease in the magnetic moments was observed for the S-bonded cobalt complexes of H_4L^1 (2.0–2.4 BM) relative to the O-bonded Co^{II} complexes of H_4L^2 (3.42–3.92 BM; the trinuclear complexes **17** and **19** are exceptions). Further evidence for the Co^{II}/Co^{III} structures is found in their visible and IR spectra as well as elemental and thermal analyses (table 4).

Table 4. Thermal analyses data (TG-DSC) for metal complexes of the two ligands.

Complex	Temperature range (°C)	% Weight loss Found (Calc.)	DSC peak (°C) Exo	DSC peak (°C) Endo	ΔH (J/g)	Lost fragment (no. of molecules)
1	37–113	5.8 (5.9)	113		−79	3 H_2O (hyd.)
	113–229	7.9 (7.8)		229	68	4 H_2O (coord.)
2	42–250	None	–	–	–	–
3	23–216	9.0 (9.1)		216	17	4 H_2O (coord.)
4	25–104	8.1 (8.3)	104		−26	$1\frac{1}{2}$ EtOH (solv.)
	104–253	8.8 (8.7)		253	17	4 H_2O (coord.)
5	32–109	11.5 (11.7)	109		−70	$2\frac{1}{2}$ EtOH (solv.)
	109–215	7.4 (7.3)		215	55	4 H_2O (coord.)
6	40–120	9.1 (9.2)	120		−84	5 H_2O (hyd.)
	120–220	3.8 (3.7)		220	408	2 H_2O (coord.)
7	44–112	4.9 (5.0)	112		−70	1 EtOH (solv.)
8	25–150	7.1 (7.3)	150		−72	$1\frac{1}{2}$ EtOH (solv.)
9	32–131	6.2 (6.2)	131		−82	$1\frac{1}{4}$ EtOH (solv.)
10	32–130	9.4 (9.5)	130		−98	2 EtOH (solv.)
11	20–138	1.7 (1.8)	138		−460	$\frac{1}{4}$ EtOH (solv.)
	138–265	11.2 (11.1)		265	126	4 H_2O (coord.)
12	31–158	4.7 (4.6)	158		−79	$2\frac{1}{2}$ H_2O (hyd.)
	158–228	5.3 (5.5)		228	86	3 H_2O (coord.)
	228–376	14.8 (14.9)		376	378	1 oxine
13	25–120	4.1 (4.2)	120		−88	1 EtOH (solv.)
	120–230	5.7 (5.9)		230	120	1 EtOH (coord.) + 1 H_2O (coord.)
	230–360	22.6 (22.4)		360	255	1 phen + 1 HNO_3 (coord.)
14	27–138	4.2 (4.4)	138		−115	$2\frac{1}{2}$ H_2O (hyd.)
	138–195	3.6 (3.5)		195	88	2 H_2O (coord.)
	195–277	21.5 (21.3)		277	172	1 Bpy + 1 HNO_3 (coord.)
15	25–130	6.6 (6.7)	130		−94	1 EtOH (solv.)
	130–252	10.7 (10.5)		252	148	4 H_2O (coord.)
16	31–102	3.5 (3.5)	102		−56	$\frac{1}{2}$ EtOH (solv.)
	102–262	10.8 (10.9)		262	358	4 H_2O (coord.)
	262–364	21.6 (21.8)		364	107	1 H_2O (coord.) + 2 HNO_3 (coord.)
17	30–115	5.2 (5.3)	115		−60	1 EtOH (solv.)
	115–189	4.1 (4.1)		189	88	2 H_2O (coord.)
18	31–155	9.9 (10.0)	155		−80	1 EtOH (solv.) + 2 H_2O (hyd.)
	155–365	16.8 (16.5)		365	125	4 H_2O (coord.) + 2 HNO_3 (coord.)
19	33–113	7.2 (7.2)	113		−90	$1\frac{1}{2}$ EtOH (solv.)
	113–265	7.6 (7.5)		265	160	4 H_2O (coord.)
20	27–105	2.7 (2.7)	105		−61	1 H_2O (hyd.)
	105–270	11.1 (11.0)		270	380	4 H_2O (coord.)
	270–351	22.1 (21.9)		351	205	1 H_2O (coord.) + 2 HNO_3 (coord.)

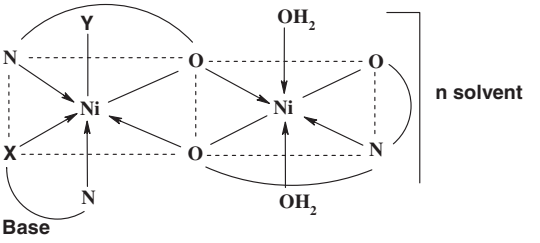

Base	X	Y	*n* solvent	Complex
oxine	O	H_2O	2.5 H_2O	**12**
phen	N	NO_3^-	1 EtOH	**13**
Bpy	N	NO_3^-	2.5 H_2O	**14**

Scheme 3. Mixed-dimeric Ni^{II} complexes of H_4L^2.

3.8. *Ni^{II} complexes (d^8-system)*

The red Ni^{II} complex **2** is diamagnetic, suggesting a square planar geometry around the Ni^{II}-ion. A weak absorption band (shoulder) at 485 nm assigned to $^1A_{1g} \rightarrow {}^1A_{2g}$ transition supports the square-planar geometry. All the other Ni^{II} complexes (**1**, **3**–**5**, **11**–**15**) showed the main O_h band as an intense broad band around 23,530 cm^{-1}, which is assigned to the $^3A_{2g}(F) \rightarrow {}^3T_{1g}(P)$ ν_3 transition. In addition, a shoulder around 20,830 cm^{-1} may be assigned to the ν_2 transition arising from $^3A_{2g}(F) \rightarrow {}^3T_{1g}(F)$. As shown in table 3, a blue shift was observed for S-bonded complexes (**1**–**5**) compared to those O-bonded (**11**–**15**). The magnetic moments of the Ni^{II} complexes (table 3) lie in the ranges 2.0–2.20 BM for S-bonded complexes and 2.83–3.32 BM for O-bonded complexes. These μ_{eff} values are indicative of two unpaired electrons and suggest a strong antiferromagnetic exchange between the adjacent Ni^{II}-cations, especially existing in dimeric structures (complexes **1**, **5**, **12**–**14**; table 3 and schemes 3 and 4). In addition, a much stronger interaction is indicated for the S-bonded compared to the O-bonded complexes (i.e. S-bridges can propagate very strong magnetic exchange and may account for the reduced magnetic moments in their Ni^{II} complexes).

3.9. *Mass spectra*

Mass spectra provide evidence for the molecular formulae of these complexes. The complexes $[(HL^1)Ni_2(Bpy)(H_2O)_5]NO_3 \cdot 1\frac{1}{2}EtOH$ (**4**) (FW 832.20) and $[(H_2L^2)(H_3L^2)Ni_2(Bpy)(NO_3)(H_2O)_2] \cdot 2\frac{1}{2}H_2O$ (**9**) (FW 1030.26) showed peaks at *m*/*e* 759 and 986, in agreement with the formulae weights of the nonsolvated complexes $[(HL^1)Ni_2(Bpy)(H_2O)_5]NO_3$ (FW 763) and $[(H_2L^2)(H_3L^2)Ni_2(Bpy)(NO_3)(H_2O)]$ (FW 985). Mass spectra of $[(H_2L^1)_2Co_2(H_2O)(NO_3)]EtOH$ (**7**) (FW 920.78) and $[(H_2L^2)_2Co_3(OH)_2]EtOH$ (**17**) (FW 869.45) showed molecular ion peaks at *m*/*e* 920.1 and 870, respectively.

3.10. *Thermal analyses (TG-DSC)*

TG-DSC studies were carried out on the ligands and their complexes at a heating rate 10°C/min in a nitrogen atmosphere (30 mL/min) over the temperature

range 20–800°C. The results (table 4) show good agreement with the theoretical formulae as suggested from the elemental analyses. H_4L^1 was found to be stable up to 130°C, and H_4L^2 up to 250°C. Greater stability of the ligands compared with their chelates suggests powerful intramolecular H-bonding in the ligands [20]. The thermograms of the chelates can be subdivided into two or three main regions depending on the nature of the chelates. (i) The first region extends up to 158°C and corresponds to the weight loss of the hydrated water molecules and/or solvated ethanol molecules during one exothermic process. (ii) The second region extends up to 288°C and corresponds to the weight loss of the coordinated water molecules during a strong

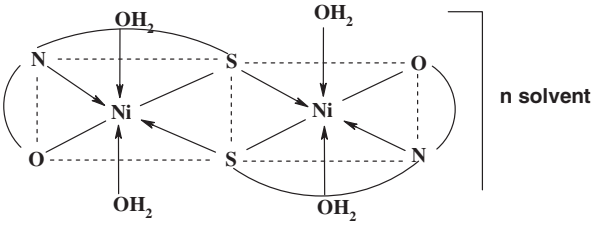

Complexes **1** and **5** (n solvent; see table 1)

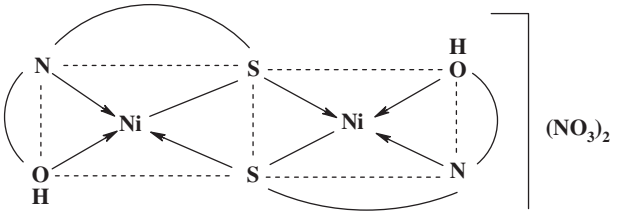

Complex **2**

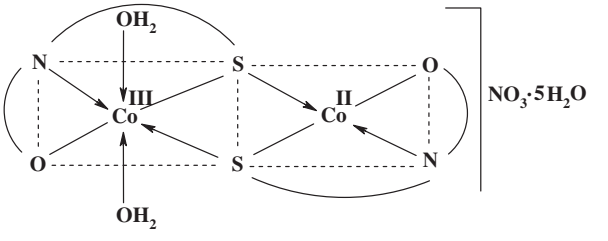

Complex **6**

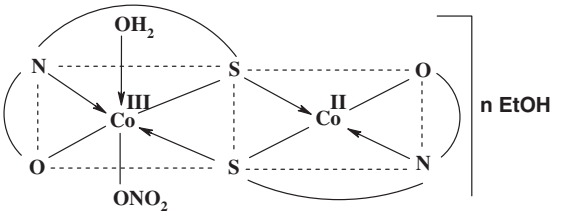

Complexes **7–10** (n EtOH; see table 1)

Scheme 4. Dimeric Ni^{II} and Co^{II}/Co^{III} complexes of H_4L^1.

endothermic process (table 4). (iii) Above 288°C, the complexes begin to decompose slowly, then more rapidly up to 800°C with the formation of Co_3O_4 and NiO. The metal content was concordant with the results of the elemental analyses. However, these general features depend on the nature of each complex. Thermogravimetry of $[(H_3L^1)_2Ni_2](NO_3)_2$ (**2**) showed no weight loss up to 250°C, indicating the absence of water/ethanol molecules in the complex. Thermogravimetry of the Co^{II}/Co^{III} complexes **7**–**10** showed that the loss of the coordinated water molecule was accompanied by the decomposition of these complexes by degradation of the organic part of the chelates (table 4).

4. General discussion

The reaction of both H_4L^1 and H_4L^2 with Co^{II} and Ni^{II} nitrates afforded dimeric complexes (**1** and **6**) in the case of H_4L^1 and binuclear complexes (**10** and **16**) in the case of H_4L^2, reflecting the higher tendency of S to form bridges than O. The dimeric cobalt complex **6** was found to be unreactive towards phen, Bpy, Tmen and oxine (scheme 4; complexes **7**–**10**). All these complexes contain side/side, Co^{II}/Co^{III} ions. Arguments supporting these Co^{II}/Co^{III} structures begin with the observation of a pronounced decrease in their μ_{eff} values, in addition to their elemental and thermal analyses and IR and visible spectra. By contrast, the dimeric Ni^{II} complex **1** showed higher reactivity towards the aromatic bases phen and Bpy. Surprisingly, in the presence of oxine, the dimeric brown paramagnetic O_h complex (**1**) was transformed to the dimeric brick–red diamagnetic square-planar complex (**2**). Complex **2** showed a ^1H NMR spectrum that was explained on the basis of H^+-transfer (scheme 2). It can be concluded that the presence of the oxine molecules in the reaction medium increases the difference in energy between the d_z^2 and $d_{x^2-y^2}$ orbitals. This energy difference

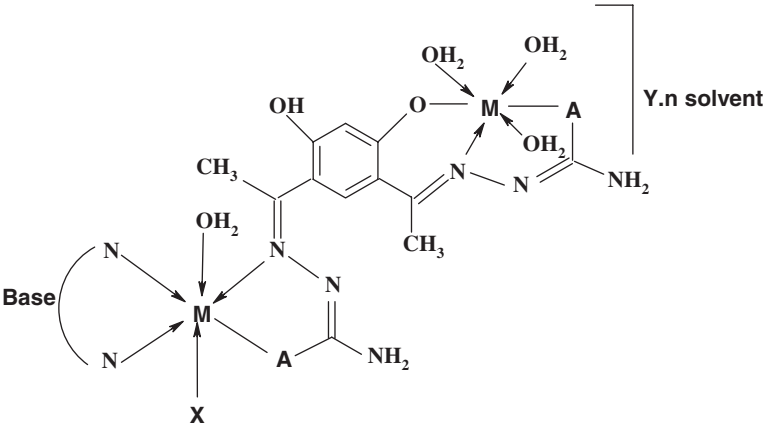

A	M	X	Y	Base	*n* solvent	Complex
S	Ni	H_2O	NO_3^-	phen	–	**3**
S	Ni	H_2O	NO_3^-	Bpy	1.5 EtOH	**4**
O	Co	NO_3^-	–	phen	2 H_2O·1 EtOH	**18**

Scheme 5. Adducts of both H_4L^1 and H_4L^2.

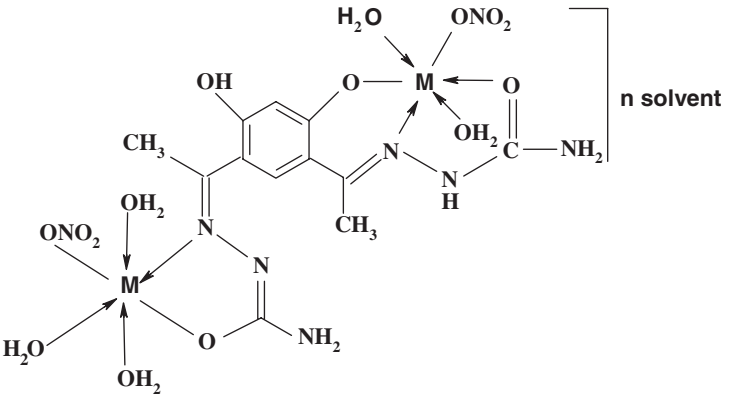

M = Ni; complexes **11**, **15** and M = Co; complexes **16**, **20** (n solvent; see table 1)

Scheme 6. Binuclear Ni^{II} and Co^{II} complexes of H_4L^2.

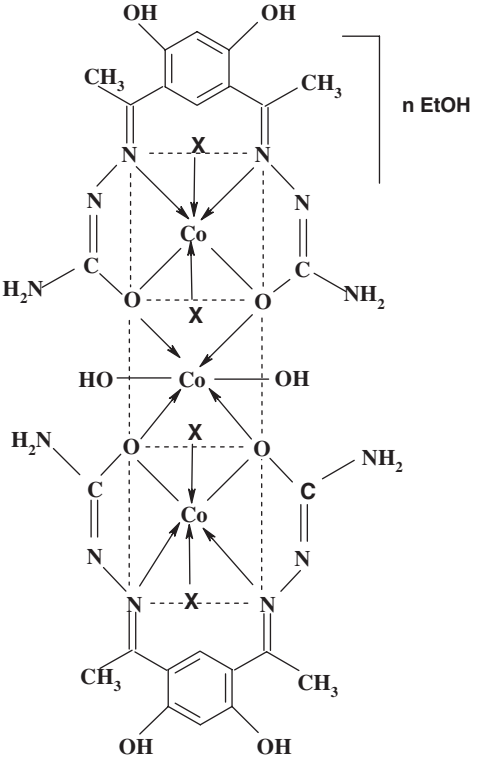

X	*n*	Complex
–	1	**17**
H_2O	1.5	**19**

Scheme 7. Trinuclear Co^{II} complexes of H_4L^2.

becomes larger than the energy needed to pair the electrons, that is the $(e_g)^2$ electrons pair up and occupy the lower energy d_z^2 orbital leaving the $d_{x^2-y^2}$ orbital empty. Under these conditions a more stable diamagnetic square-planar arrangement arises (complex **2**). Furthermore, the reactivity of the binuclear Ni^{II} complex (**11**) towards phen, Bpy and oxine afforded mixed dimeric complexes with the mole ratio 2 : 2 : 1 (Ni^{II} : H_4L^2 : base) (scheme 3; complexes **12**–**14**). Interaction of H_4L^2 with Co^{II} nitrate in the presence of oxine and Bpy afforded trinuclear complexes in which the ligand squeezes its ONNO compartments to generate cavities of the right size to accommodate three Co^{II} ions via O-bridging (scheme 7; complexes **17**, **19**). In the case of phen, the reaction afforded a 2 : 1 : 1 Co^{II} : H_4L^2 : phen adduct. Finally, all of the complexes were unreactive towards the aliphatic base Tmen. This may be attributed to the presence of four bulky methyl groups attached directly to the coordinating sites of Tmen.

In conclusion, binuclear, dimeric, trinuclear, mixed dimeric and mixed-ligand binuclear complexes have been obtained, depending on the nature of the ligand (S or O containing) and the metal ion (Co^{II} or Ni^{II}). The ligands show various modes of bonding that may be attributed to the different tautomeric forms and the higher tendency of O and especially S to form bridges. Based on the above results, the proposed structures of the complexes are given in schemes 3–7.

References

[1] S.E. Livingstone, *Q. Rev.* **7**, 59 (1971).
[2] M.J.M. Campbell, *Coord. Chem. Rev.* **15**, 279 (1975).
[3] P. Souza, A.I. Matesan, V. Fernandez, *J. Chem. Soc., Dalton Trans.* 3011 (1996).
[4] D.X. West, A.E. Liberta, S.B. Padhye, R.C. Chikate, P.B. Sonawane, A.S. Kumbhar, R.G. Yerande, *Coord. Chem. Rev.* **123**, 49 (1993).
[5] D.X. West, S.B. Padhye, P.B. Sonawane, *Struct. Bonding* **76**, 1 (1991).
[6] S. Padhye, G.B. Kauffman, *Coord. Chem. Rev.* **63**, 127 (1985).
[7] H.S. Seleem, *Annal. Chim.* **93**, 305 (2003).
[8] H.S. Seleem, B.A. El-Shetary, S.M.E. Khalil, M. Shebl, *J. Serbian Chem. Soc.* **68**, 729 (2003).
[9] S.M.E. Khalil, H.S. Seleem, B.A. El-Shetary, M. Shebl, *J. Coord. Chem.* **55**, 883 (2002).
[10] H.S. Seleem, M. El-Behairy, M. Mashaly, H. Mena, *J. Serbian Chem. Soc.* **67**, 243 (2002).
[11] O.P. Pandey, *Polyhedron* **6**, 1021 (1987).
[12] C. He, C.Y. Duan, C.J. Fang, Y.J. Liu, Q.J. Meng, *J. Chem. Soc., Dalton Trans.* 1207 (2000).
[13] K. Nakamoto, In *Infrared and Raman Spectra of Inorganic and Coordination Compounds*, 5th Edn, John Wiley & Sons, USA (1997).
[14] C. Yan, Y. Li, *Synth. React. Inorg. Met.-Org. Chem.* **30**, 99 (2000).
[15] E. Spodine, Y. Moreno, M. Garland, O. Pena, R. Baggio, *Inorg. Chim. Acta* **309**, 57 (2000).
[16] S. Yu, Q. Wang, B. Wu, X. Wu, H. Hu, L. Wang, A. Wu, *Polyhedron* **16**, 321 (1997).
[17] S. Yu, Q. Huang, B. Wu, W. Zhang, X. Wu, *J. Chem Soc., Dalton Trans.* 3883 (1996).
[18] J. Zhang, W. Zhang, Q. Luo, Y. Mei, *Polyhedron* **18**, 3637 (1999).
[19] C.K. Choudhary, R.K. Choudhary, L.K. Mishra, *J. Indian Chem. Soc.* **80**, 693 (2003).
[20] V. Mishra, *J. Indian Chem. Soc.* **79**, 374 (2002).